

REPORT DOCUMENTATION PAGE			<i>Form Approved</i> <i>OMB No. 0704-0188</i>	
Public reporting burden for this collection of information is estimated to average 1 hour per response, including the time for reviewing instructions, searching existing data sources, gathering and maintaining the data needed, and completing and reviewing this collection of information. Send comments regarding this burden estimate or any other aspect of this collection of information, including suggestions for reducing this burden to Department of Defense, Washington Headquarters Services, Directorate for Information Operations and Reports (0704-0188), 1215 Jefferson Davis Highway, Suite 1204, Arlington, VA 22202-4302. Respondents should be aware that notwithstanding any other provision of law, no person shall be subject to any penalty for failing to comply with a collection of information if it does not display a currently valid OMB control number. PLEASE DO NOT RETURN YOUR FORM TO THE ABOVE ADDRESS.				
1. REPORT DATE (DD-MM-YYYY) March 14, 2012		2. REPORT TYPE Final Progress Report		3. DATES COVERED (From - To) September 15, 2010 - December 14, 2011
4. TITLE AND SUBTITLE ACQUISITION OF MECHANICALLY ASSISTED SPARK PLASMA SINTERING SYSTEM FOR ADVANCED RESEARCH AND EDUCATION ON FUNCTIONALLY GRADED HYBRID MATERIALS			5a. CONTRACT NUMBER	
			5b. GRANT NUMBER FA9550-10-1-0398	
			5c. PROGRAM ELEMENT NUMBER	
6. AUTHOR(S) Dimitris Lagoudas, Miladin Radovic, Ibrahim Karaman			5d. PROJECT NUMBER	
			5e. TASK NUMBER	
			5f. WORK UNIT NUMBER	
7. PERFORMING ORGANIZATION NAME(S) AND ADDRESS(ES) Texas Engineering Experiment Station 1470 William D. Fitch Pky College Station, TX 77843			8. PERFORMING ORGANIZATION REPORT NUMBER	
9. SPONSORING / MONITORING AGENCY NAME(S) AND ADDRESS(ES) Air Force Office of Scientific Research Suite 325, Room 3112 875 Randolph Street Arlington, VA 22203-1768			10. SPONSOR/MONITOR'S ACRONYM(S) AFOSR	
			11. SPONSOR/MONITOR'S REPORT NUMBER(S) AFRL-OSR-VA-TR-2012-0940	
12. DISTRIBUTION / AVAILABILITY STATEMENT Distribution A - Approved for Public Release				
13. SUPPLEMENTARY NOTES				
14. ABSTRACT This is the final progress report of activities at Texas Engineering Experiment Station (TEES)/Texas A&M University (TAMU) on work related to the AFOSR – Defense University Research Instrumentation Program (DURIP) Project titled, "Acquisition of Mechanically Assisted Spark Plasma Sintering System for Advanced Research and Education on Functionally Graded Hybrid Materials". The effective beginning date of Contract No. FA9550-10-1-0398 was September 15, 2010. The project was aimed at developing facilities for pressure-assisted fabrication of hybrid materials by spark plasma sintering (SPS) of metallic and ceramic powders to support a wide range of research AFOSR activities that cannot be easily achieved using existing facilities at Texas A&M University, including MURI project entitled "Synthesis, Characterization, and Prognostic Modeling of Functionally Graded Hybrid Composites for Extreme Environments". Several different components were acquiring, installed and tested the proposed systems have been successfully installed at Texas A&M University. Different MAX phases, as well as their composites with the Shape Memory Alloys (SMA) have been fabricated and they demonstrated unprecedented mechanical damping due to residual stresses in MAX phases induced by the shape memory effect. In addition, the SPS was used to join ceramics (MAX phases) to the SMA (NiTi) and study the kinetics of the interfacial reactions. The acquired SPS fabrication system is one of the most powerful in the academia and will allows us to systematically fabricate and study structural, physical and mechanical properties of these hybrid materials.				
15. SUBJECT TERMS				
16. SECURITY CLASSIFICATION OF:			17. LIMITATION OF ABSTRACT UU	18. NUMBER OF PAGES 24
a. REPORT U	b. ABSTRACT U	c. THIS PAGE U		
				19b. TELEPHONE NUMBER (include area code) 703-696-6961

Texas A&M University/Texas Engineering Experiment Station

Final Progress Report to AFOSR on the project FA9550-10-1-0398

**“ACQUISITION OF MECHANICALLY ASSISTED SPARK PLASMA SINTERING
SYSTEM FOR ADVANCED RESEARCH AND EDUCATION ON FUNCTIONALLY
GRADED HYBRID MATERIALS”**

For the Period of September 15, 2010 - December 14, 2011

Submitted to:

**Dr. David S. Stargel
Air Force Office of Scientific Research
Aerospace, Chemical and Material Sciences Directorate
Structural Materials Program**

By

**Dimitris Lagoudas, Aerospace Engineering, Texas A&M University
Miladin Radovic, Mechanical Engineering, Texas A&M University
Ibrahim Karaman, Mechanical Engineering, Texas A&M University**

March 14, 2012

Texas A&M University/Texas Engineering Experiment Station

Final Progress Report to AFOSR on the project FA9550-10-1-0398

“ACQUISITION OF MECHANICALLY ASSISTED SPARK PLASMA SINTERING SYSTEM FOR ADVANCED RESEARCH AND EDUCATION ON FUNCTIONALLY GRADED HYBRID MATERIALS”

FOREWORD

This is the final progress report of activities at Texas Engineering Experiment Station (TEES)/Texas A&M University (TAMU) on work related to the AFOSR – Defense University Research Instrumentation Program (DURIP) Project titled, “Acquisition of Mechanically Assisted Spark Plasma Sintering System for Advanced Research and Education on Functionally Graded Hybrid Materials”. The effective beginning date of Contract No. FA9550-10-1-0398 was September 15, 2010. The project was aimed at developing facilities for pressure-assisted fabrication of hybrid materials by spark plasma sintering (SPS) of metallic and ceramic powders to support a wide range of research AFOSR activities that cannot be easily achieved using existing facilities at Texas A&M University, including MURI project entitled “Synthesis, Characterization, and Prognostic Modeling of Functionally Graded Hybrid Composites for Extreme Environments”. Several different components were acquiring, installed and tested the proposed systems have been successfully installed at Texas A&M University. Different MAX phases, as well as their composites with the Shape Memory Alloys (SMA) have been fabricated and they demonstrated unprecedented mechanical damping due to residual stresses in MAX phases induced by the shape memory effect. In addition, the SPS was used to join ceramics (MAX phases) to the SMA (NiTi) and study the kinetics of the interfacial reactions. The acquired SPS fabrication system is one of the most powerful in the academia and will allows us to systematically fabricate and study structural, physical and mechanical properties of these hybrid materials.

Statement of the Problem Studied

The goal of this DURIP project has been to develop a pressure-assisted spark plasma sintering (SPS) system for developing new hybrid (metal/ceramic) materials for high temperature applications with unprecedented mechanical damping, oxidation resistance, fracture toughness, and damage tolerance. The results obtained using this system were critical for the success of the AFOSR funded research project on the development and characterization of hybrid material systems for extreme environments entitled “MURI: Synthesis, Characterization, and Prognostic Modeling of Functionally Graded Hybrid Composites for Extreme Environments” (FA-9550-09-1-0686). The main objective of the MURI project is to develop, characterize, and model multifunctional Functionally Graded (ceramic-metal-polymer) Hybrid Composites (FGHC), **Figure 1**, through collaborative research of faculties and researchers from Texas A&M University, University of Illinois at Urbana-Champaign, Virginia Polytechnic Institute and State University, Stanford University, University of Michigan, and University of Dayton Research Institute. The proposed effort offers a multidisciplinary research program to

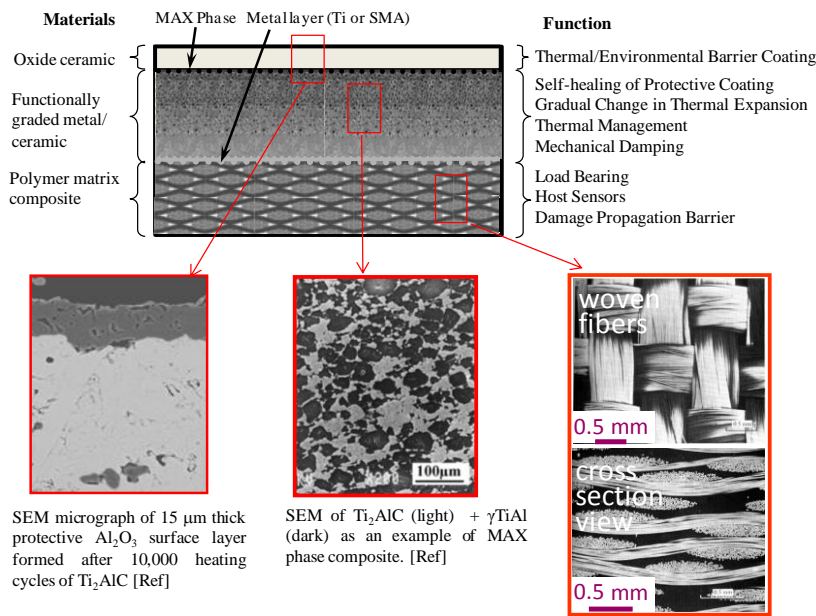
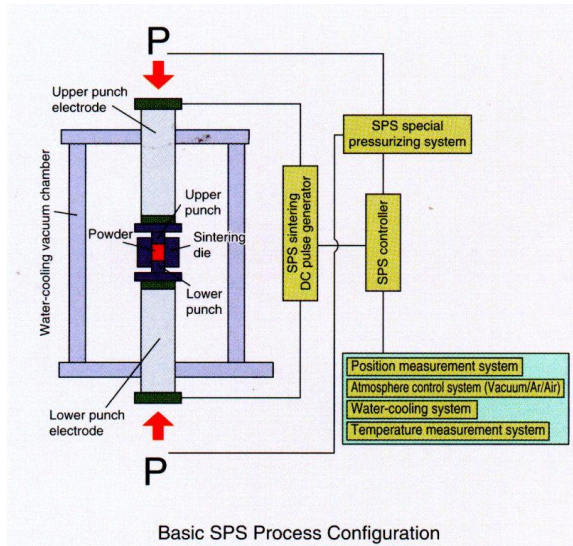


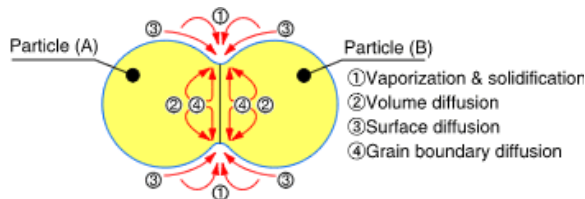
Figure 1: Schematic of the laminated functionally graded hybrid composite for 300°C - 1000 °C environment.

achieve the topic goals by coupling thermal-acoustic-mechanical flight loads to design functionally graded multifunctional hybrid material systems with integrated sensing capabilities for extreme environments that synergistically enables the development of critical structural elements such as wing surfaces, leading

edges, and turbine blades for aerospace vehicles. Such a comprehensive research effort is crucial for the development of the multifunctional hybrid composites that combine the best attributes of ceramics, metals and polymer composites with sensing and remaining-life prognosis capabilities for future Air Force flight platforms that will operate in extreme conditions over a wide range of speeds for extended periods of time.



(a)



(b)

Figure 2. (a) A schematic of the SPS sintering setup, (b) various material transfer paths during sintering.

To be able to achieve our goal of designing hybrid material structures with optimized multifunctional properties for extreme environments, we first needed to understand - on the fundamental level - how composition and architecture of, and interfaces in, hybrid materials of the choice affect their physical and mechanical properties. Then, with this understanding, we were able to perform a well-structured experimental program optimizing the structure and composition of FGHC to optimize their multidisciplinary performance. However, this is not a trivial task since it requires a large number of fabrication experiments that are in general time consuming if conventional methods, such as molten metal infiltration in ceramic preform with functionally graded porosity or co-sintering of metallic-ceramic powders, are to be used to process different FGHCs. Therefore, fabrication of FGHCs using SPS (**Figure 2**) is crucial because it **allows a rapid synthesis** and densification of single-phase bulk materials and hybrid composites with various compositions and architecture. Short sintering times that can be achieved using SPS as well as melting of surfaces without heating the interior of

the powder particles prevent eventual chemical reaction between dissimilar materials and allows fast processing of different samples unlike labor intensive and time consuming processing such as melt infiltration and co-sintering. Additional advantages of using SPS system for processing of FGHCs over conventional techniques are summarized below:

- **Better control of phase distribution in composites** – Sluggish kinetic of grain growth during SPS allows better control of phase distribution and size of each phase. Different phase distribution and morphology can be simply achieved by varying particle sizes of initial powders.
- **Lowering the co-sintering temperature**– SPS sintering can be achieved usually at temperatures 300-500 °C lower than conventional processes such as hot pressing, hot isostatic pressing, and pressure-less sintering. This is of crucial importance to prevent uncontrolled grain growth of undesirable phases or eventual chemical reactions between dissimilar materials.

- **Gradual phase transition in composites** – SPS allows easy processing of the functionally graded composite samples with more gradual change in phase composition, when compared to other conventional methods.
- **Homogeneous and fully dense composites** – SPS allows the formation of fully dense composites unachievable with other conventional methods. For example, melt infiltration of metallic phase in the ceramic preform with functionally graded porosity could result in incomplete filling of all pores with molten metal especially if these pores are closed and not interconnected. Consequently, the final product would have significant inbuilt residual porosity.
- **Joining of the dissimilar materials** – SPS also facilitates the joining of dissimilar materials and processing of the samples for studying structure and properties of the interfaces between different phases.

The acquired SPS system includes the following five main components and accompanying measurement systems: (1) sintering unit, (2) analysis unit, (3) high vacuum system, (4) the radiation thermometry, and (5) cooling water recirculation system. The sintering unit consists of a tie-bar frame with a vertical single axis hydraulic cylinder that allows loads from 5 kN to 25 tons. The stroke of the cylinder is 6". The pressure control system includes a feedback control by proportional solenoid relief valve where the pressure is measured using a strain gage pressure transducer. The DC pulse generator which is a part of the sintering unit has a maximum output current of 10000 Amps. The control system includes automatic and manual control modes with digital timer and automatic closed loop program. The sintering chamber allows sintering in vacuum (5×10^{-5} Torr) or inert gas environment. The state-of-the-art analysis unit includes a specimen displacement measuring unit, pressure program control unit, sintering data analysis software and an external output terminal. The temperature is measured using an infrared radiation thermometer up to 2200 °C.

The acquired instruments provide a dedicated, convenient, and efficient facility for a wide range of materials, composites, and functionally graded hybrid materials systems. Since the SPS method is an emerging and promising fabrication technology for novel materials and forms, the further utilization of this method for metals, ceramics, polymers, and functionally graded hybrids in U.S. will be beneficial for the Air Force applications. Texas A&M already has extensive facilities for the fabrication of bulk and porous metals and ceramics using powder metallurgy methods such as: high-temperature pressureless sintering, hot pressing, hot isostatic pressing facilities, cold pressing, tape casting, etc. The addition of the proposed equipment complement the existing facilities, fill a big gap in TAMU's materials fabrication capabilities and provide a unique opportunity for developing new materials and structures that are of importance for Air Force systems. In addition, this is the first SPS system available in the academia in the State of Texas, and even more the most powerful research scale SPS system in an academic institution nationwide.

The accrued system has also enhanced the research-related educational opportunities for undergraduate and graduate engineering students by being generally available to at least three faculty and their students. Four graduate students and one visiting scholar have been trained to process different materials using SPS. In addition,

it has been used as a demonstrational facility in “Fundamentals of Ceramics” (MEEN 658 and MSEN 658) course in Spring 2012 by one of Co-PIs (M. Radovic).

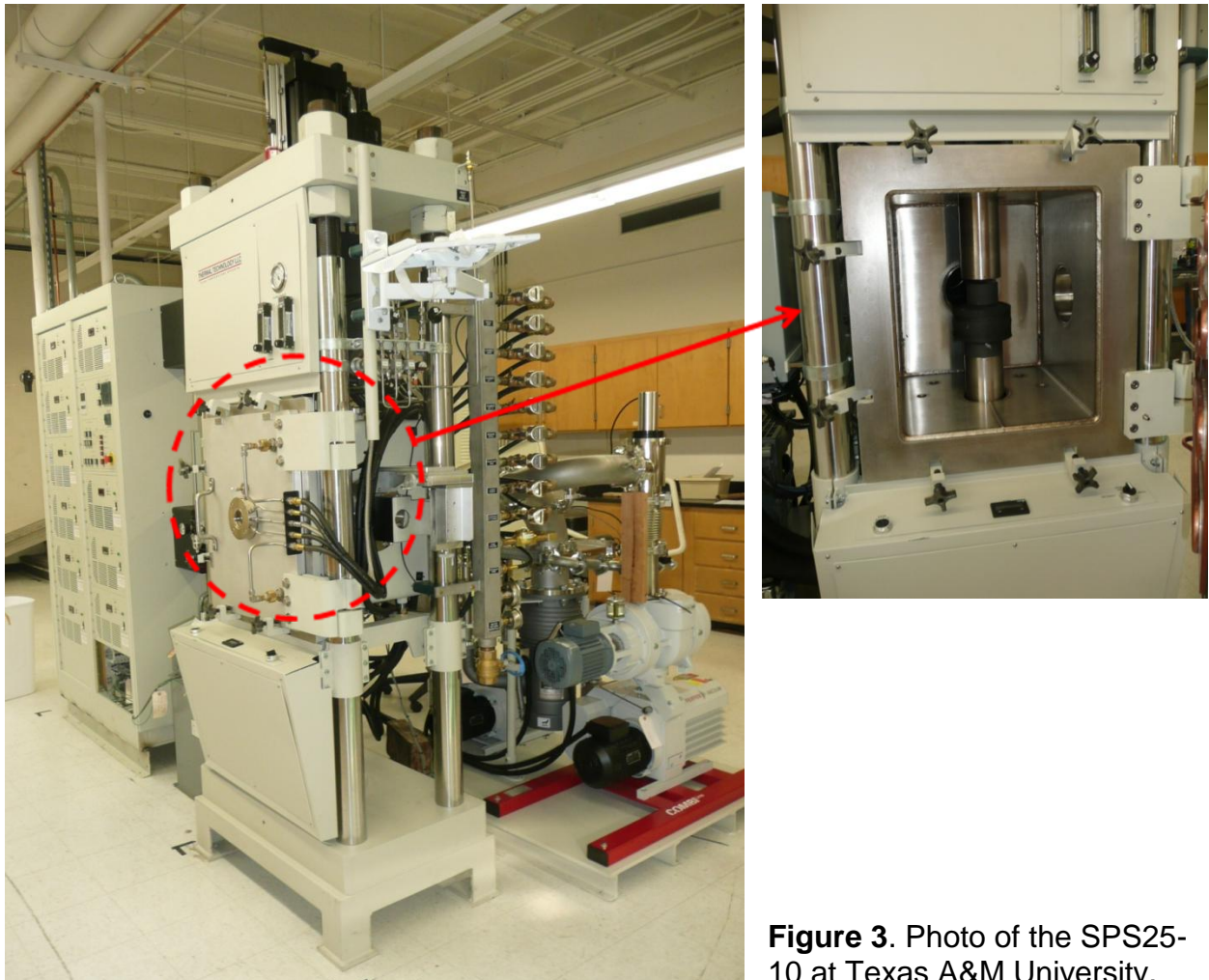


Figure 3. Photo of the SPS25-10 at Texas A&M University.

Summary of Most Important Results

The SPS 25-10 system has been acquired from Thermal Technology LLC and installed at Materials Fabrication and Characterization Center at Texas A&M University. As of Fall 2011, the SPS system has been successfully used to fabricate fully dense ceramics (MAX phases), ceramic-metal composites, as well as to join ceramics to metals. The details of the individual components of the SPS system and structural and mechanical properties of the materials that were processed by the acquired system are presented below.

Acquisition and Installation of SPS25-10 Unit

The acquired SPS system, namely SPS25-10 (Thermal Technology LLC, CA) is shown in the **Figure 3**, while detail specification of the equipment are provided in the **Table 1**.

Table 1. Specification of the SPS25-10.

Subsystem:	Descriptions
SYSTEM GENERAL SPECIFICATIONS	<ul style="list-style-type: none"> • Maximum operating temperature: 2200°C • Pressing Capability: 25 ton total force • Ultimate Vacuum Level: 10⁻⁵ torr • Process Gasses Used: Argon, Nitrogen, or Helium • Pressing Capability: 25 ton total force.
CHAMBER ASSEMBLY	<ul style="list-style-type: none"> • Front loading, rectangular chamber. Inside chamber dimensions 17" x 17" x 20". One (1) 2.0" (50mm) inside diameter sight window. • Blanked port for optional optical pyrometer. • Single port for standard (mechanical vacuum pump) and high vacuum system.
POWER SUPPLY	<ul style="list-style-type: none"> • 10,000 amp, 10 VDC pulsed power supply. • Minimum 4 msec on time pulse to maximum 999 msec on time pulse. • Minimum 0 msec off time pulse to 999 msec off time pulse. • Square wave form ("on" and "off" time) are manually adjustable and programmable with a PC (supplier supplied). • Current or voltage mode operation. • Waveform control changes may be initiated during a run. • Robust switching power supply design with high frequency power transformers and IGBT's for fast, clean waveforms. • Ammeter and voltmeter to read average output amps and volts.
VACUUM SYSTEM	<ul style="list-style-type: none"> • Pfeiffer Model WD 400 Roots Pump Unit, 470 m³/hr (153 cfm) volume flow rate with OKTA 500 A Roots Pump and DUO 65 Rotary Vane Pump, Oil Mist Filter, Oil Return, and Safety Valve • One (1) electro-pneumatically operated roughing valve. • Spool pieces, O-rings, seals, supports and miscellaneous hardware. • Tank release valve, etc. • Air manifold system used to operate pneumatic valves. • Miscellaneous hardware and plumbing to complete vacuum manifold.
HIGH VACUUM SYSTEM	<ul style="list-style-type: none"> • VACUUM SYSTEM (10⁻⁶ torr cold, clean, dry and empty) • Edwards Diffstak Model VS160S 6" Diffusion pump

	<p>package.</p> <ul style="list-style-type: none"> • Leybold roughing pump. • One (1) electro-pneumatic operated high vacuum valve. • One (1) electro-pneumatically operated roughing valve. • One (1) electro-pneumatically operated foreline valve. • Spool pieces, O-rings, seals, supports and miscellaneous hardware. • Tank release valves, etc. • Air manifold system used to operate pneumatic valves. • Vacuum gauging. • Miscellaneous hardware and plumbing to complete vacuum manifold. • One (1) digital vacuum instrument (range 1×10^{-1} to 1×10^{-9} torr) with 3/4" diameter hot filament ion gauge tube and two (2) thermocouple gauges.
HYDRAULIC PRESS SYSTEM FOR 25 TON OPERATION	<ul style="list-style-type: none"> • 25 ton, four (4) rigid-post and platen load frame with threaded post to aid in ram alignment. • • One (1) hydraulic cylinder, top mounted (6" stroke). • Hydraulic power supply includes pump, oil reservoir, filters, etc. • Proportional pressure control valve for manual and programmed pressure control operation with miscellaneous valves, manifold and pressure gauge indicators
PROCESS GAS SYSTEM	<p>The inert gas control includes a panel-mounted flow meter, a solenoid actuated isolation valve and a compound pressure gauge. All appropriate inter-component connecting plumbing is provided.</p>
CONTROLS AND INSTRUMENTATION	<ul style="list-style-type: none"> • Free-standing control cabinet painted Thermal Technology beige. • Furnace controls are all centralized on front of cabinet for ease of operation. • Eurotherm Model 2704 high performance controller/programmer with up to 20 programs. One channel will be used to create closed-loop control of temperature. A second channel to maintain closed-loop control of force with a load cell as the feedback element. • Ram position read out will be displayed. • A PC for temperature, force and waveform profiling and data acquisition will be provided. • Data acquisition provided with SpecView software: Force, Z axis (ram) position, Temperature, Vacuum (chamber pressure), Voltage, Amperage
TEMPERATURE CONTROL SYSTEM	<ul style="list-style-type: none"> • Ten (10) Type K and five (5) Type C thermocouples with protective flexible sheaths.

	<ul style="list-style-type: none"> • Optical Pyrometer, Adjustable Flange, and Monitor: <ul style="list-style-type: none"> ○ Raytek one color optical pyrometer with optical head. Useful range 540°C - 3000°C ○ Window assembly and mounting with X,Y,Z axis manual movement. ○ Video monitor with bracket.
WATER SYSTEM	<ul style="list-style-type: none"> • Safety flow interlock sensors on critical water circuits – protection in low-flow and no-flow conditions. • Water manifolds, one for supply and one for discharge. • Manual valves for flow adjustment of water circuits. • Haskris WW4 Non-Refrigerated Water Recirculating Systems
TOOLING	<ul style="list-style-type: none"> • Five (15) sets of 20 mm dies • Five (5) sets of 40 mm dies • One (1) set of 60 mm dies • One (1) of spacers for each: 20, 40 and 60 mm dies

The SPS25-10 from Thermal Technology LLC was selected after collecting bids, among 6 different systems because this vendor offered the most powerful system together with the best training and service condition. In addition, Thermal Technology was the only vendor that has service teams and customer service in U.S.A., and those can provide a prompt help if needed. One of the PIs, namely Dr. Radovic has spent four days in June 2011 at Thermal Technology LLC, where he got trained to use the equipment. In addition, 3 graduate students have been trained to operate SPS25-10 by Thermal Technology's staff at Texas A&M University.

Table 2. Dynamic of the project realization.

Dates:	Descriptions of activity
September 15, 2010 – November 15, 2010	Contacting all potential vendors and discussing potential systems
November 20, 2010	Opening the bid
January 4, 2011	Requiring additional bid information from potential vendors on the water cooling system
February 11, 2011	Placing an order – expected delivery date July 15, 2011
July 15, 2011	Extending delivery date upon vendors request
September 7, 2011	Receiving SPS25-10
September 14-15, 2011	Moving components of the SPS25-10 Damaging load frame during moving by ATLAS MACHINERY MOVERS, INC.
October 19-21, 2011	Commissioning, installation and testing of the equipment by vendor. The system was ready for limited use until all damages are fixed.
November 28-30, 2011	Repair of the damages introduced during moving and realignment of the loading frame
November 30, 2011	SPS25-11 is fully operational.

The dynamic of the acquisition and installation of the SPS25-10 system is provided in the **Table 2**. It is worth noting here that the full installation of the SPS system was delayed for the two main reasons. First, the vendor was near 2 months late with delivery. Second, the loading frame was damaged during moving to the laboratory by professional riggers, and thus it was not possible to use it to the full extend after installation. This damage was fixed on the expense of the mover and their insurance. Regardless of unanticipated delays in the delivery and full utilization of the SPS system, we were able to process different ceramic and ceramic-metal composites and characterize their properties. More detail on that is provided in the following sections.

Spark-Plasma Sintering of the MAX Phases

The SPS25-10 system has been utilized to sinter fully dense MAX phase ceramics from MAX phase powders. When compared to other traditional processing routes such as pressureless sintering or pressure-assisted sintering such as hot pressing (HPing) and hot isostatic pressing (HIPing), where the sample is heated externally by convection and radiation, spark plasma sintering heats the sample internally, significantly reducing processing time from hours to minutes. Moreover, the powders are compacted during the sintering process via hydraulic actuated load ram, to assist the densification of the powder compacts. Besides reducing time and energy, greater control of the morphology is obtained due to the extremely fast heating rates and subsequent cooling rates of up to 200°C/min achievable by SPS.

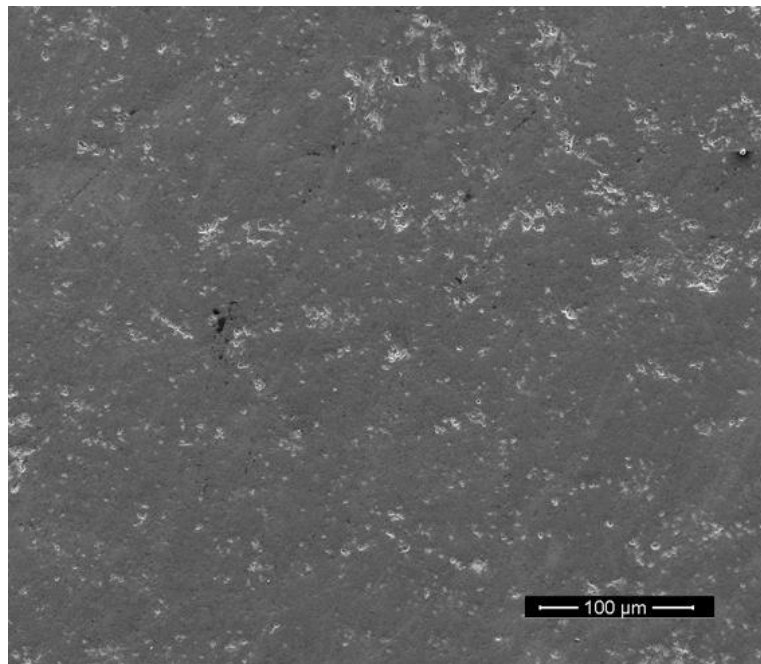


Figure 3: Ti₂AlC sintered at 1200°C for 30 min with relative density of ~ 97%.

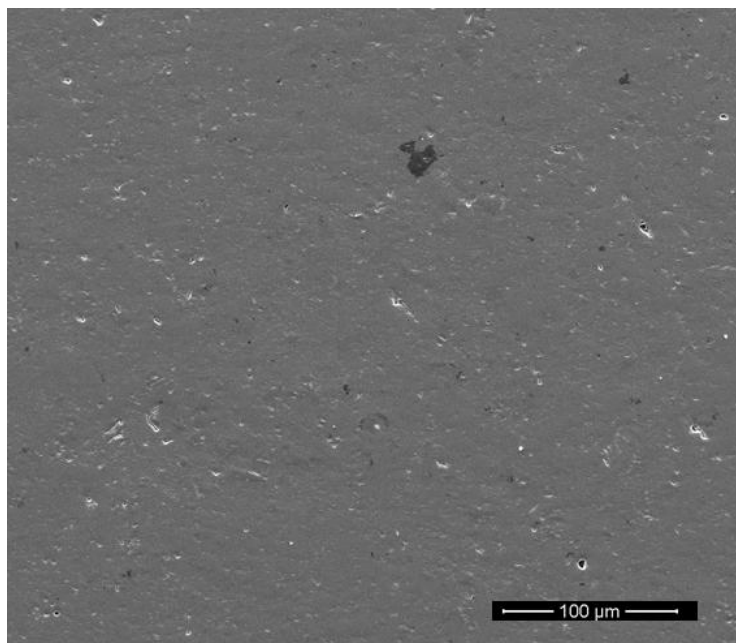


Figure 4: Ti_3SiC_2 sintered 1450°C for 6 min, notice very low porosity of sample

Since acquisition of SPS system, MAX phase samples of Ti_3SiC_2 and Ti_2AlC have been successfully sintered from MAX phase powders using SPS. **Figure 3** and **Figure 4** show Scanning Electron Microscopy images of the sintered samples. SPSing conditions for sintering of Ti_2AlC include heating the powders at $200^\circ\text{C}/\text{min}$ to temperatures in the range of $1,000^\circ\text{C}$ to $1,300^\circ\text{C}$ and with soak times in the range of 6 minutes to a maximum of 40 minutes under a constant pressure of 50 – 100 MPa. By monitoring the load ram displacement during sintering, the real-time shrinkage, or densification of the sample may be analyzed such that the optimal processing parameters may be determined quickly and effectively. Through the optimization of these processing parameters, Ti_2AlC samples with relative densities higher than 99% have been synthesized with high purity, **Figure 53 and 5**, in only 30 minutes at temperatures that are on average 200°C lower than those required in conventional sintering. Processing of Ti_3SiC_2 is generally done at higher temperatures, and thus it was studied on a much wider temperature range, from the low temperatures of 1000°C to maximum of 1450°C . These samples were also heated at $200^\circ\text{C}/\text{min}$ with soaking times from 6 minutes to 40 minutes while applying pressure of 50 - 100 MPa; maximum relative density achieved for Ti_3SiC_2 is 99.8% with very good purity, **Figure and 6**.

Currently, our goal is shifting from sintering MAX phases from MAX phase powders, to their reactive-sintering using elemental powders i.e. Ti, Al, Si, C or other common binary compounds such as TiC, SiC. In addition to the reduction of cost of raw materials and the reduction in lead time necessary to obtain MAX phase powders, this will result in higher purity samples which are currently limited by the quality of MAX phase powders obtainable today. Reactive sintering of MAX phases has been performed on site in a hot isostatic press in the past, but runtimes in excess 12 hours are required and have resulted in a limiting factor to optimize processing conditions.

However, with SPS system, an average of 5 samples have been processed in the same time span resulting in a great improvement over past capabilities. Moreover, the ability of SPS not only to heat, but also to cool at very high rates will enable to “pause” the reaction-sintering at critical steps, resulting in better understanding of the reaction mechanisms taking place.

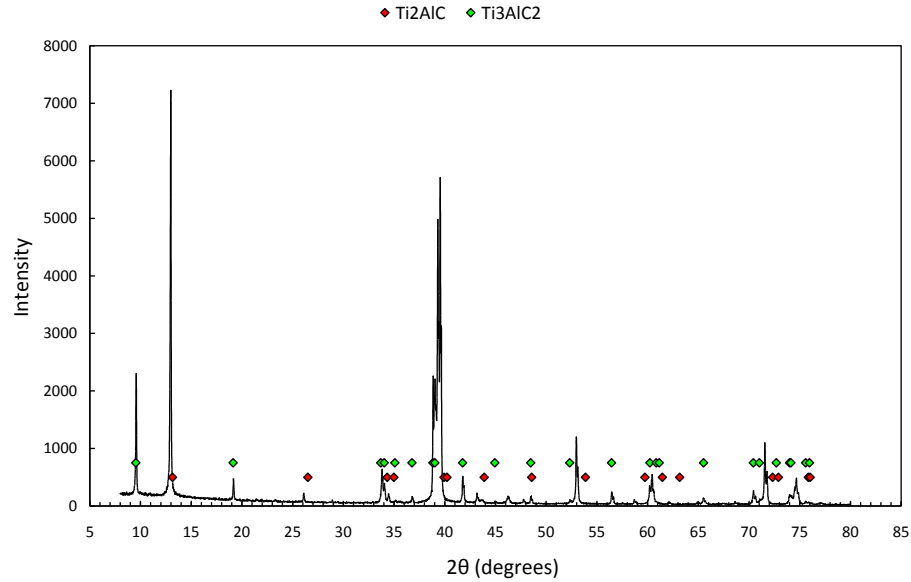


Figure 5. X-ray diffraction spectra of Ti_2AlC sintered at $1250^{\circ}C$ for 40 minutes.

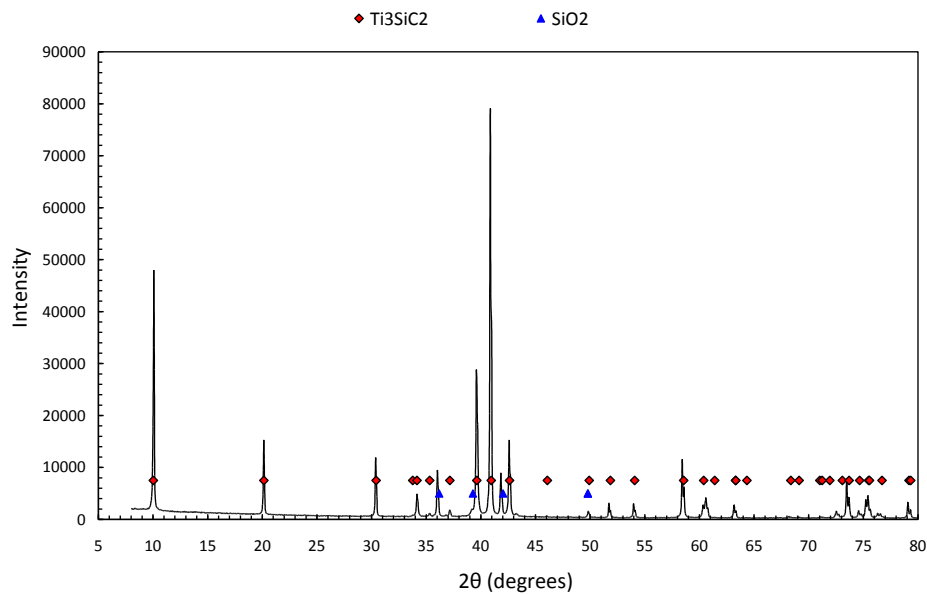


Figure 6. X-ray Diffraction spectra of Ti_3SiC_2 processed at $1450^{\circ}C$ for 6 minutes.

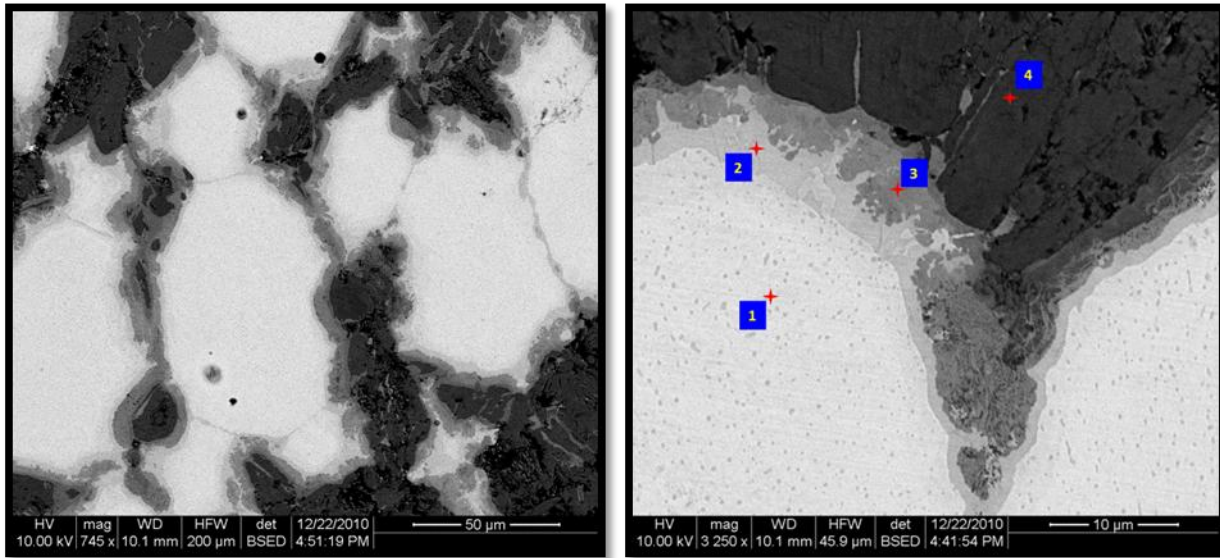
SPS Processing and Microstructural Characterization of NiTi - MAX Phase Composites

A series of NiTi - MAX phase composites were processed by spark plasma sintering (SPS) system at different conditions. **Table 3** gives some typical processing conditions for the samples that we further used for thermo-mechanical characterization (see below).. Starting powders used in this study were NiTi (Crucible Research Corporation), Ti₂AlC and Ti₃SiC₂ powders (Kanthal AB, Sweden). The NiTi powder had a composition of 50 atom.% Ni and 50 atom.% Ti and a particle size of ~20 μm. The Ti₂AlC and Ti₃SiC₂ powders were sieved and had particle size of 45 ~ 90 μm, respectively. The Ti₂AlC and Ti₃SiC₂ powders were mixed with 50 vol.% of NiTi by balling milling, respectively. The powder mixtures were poured and wrapped in graphite foil and were placed in a graphite die, followed by SPSing. During SPSing, the chamber was evacuated to 10⁻⁶ torr for 10 minutes and subsequently backfilled with argon to a pressure of 2 psi. Next, the sample was heated at 200 °C/min to 960 ~ 1100 °C and held at the target temperature for 3 ~ 30 minutes. A pressure of 100 MPa was applied before heating the powders and maintained throughout the run and until the sample was cooled to room temperature.

Table 3. Sample name, materials, sintering temperature and time, pressure, density, and porosity of NiTi – MAX phase composite samples.

Sample	Material	Sintering temperature (oC)	Time (min)	Pressure (MPa)	Density (g/cm ³)	Porosity (vol. %)
A-11	Ti ₂ AlC + NiTi	1000	5	100	-	-
A-12	Ti ₂ AlC + NiTi	1000	5	100	-	-
A-13	Ti ₂ AlC + NiTi	1000	3	100	-	-
A-14	Ti ₂ AlC + NiTi	960	20	100	-	-
A1	Ti ₂ AlC + NiTi	1100	5	100	5.09	3.6
A2	Ti ₂ AlC + NiTi	980	10	100	4.72	10.5
A3	Ti ₂ AlC + NiTi	960	30	100	4.81	8.9
A4	Ti ₂ AlC + NiTi	1000	3	100	4.71	10.8
B1	Ti ₃ SiC ₂ + NiTi	960	20	100	4.61	15.9
B2	Ti ₃ SiC ₂ + NiTi	980	10	100	4.61	15.9
B3	Ti ₃ SiC ₂ + NiTi	1000	3	100	4.5	17.9

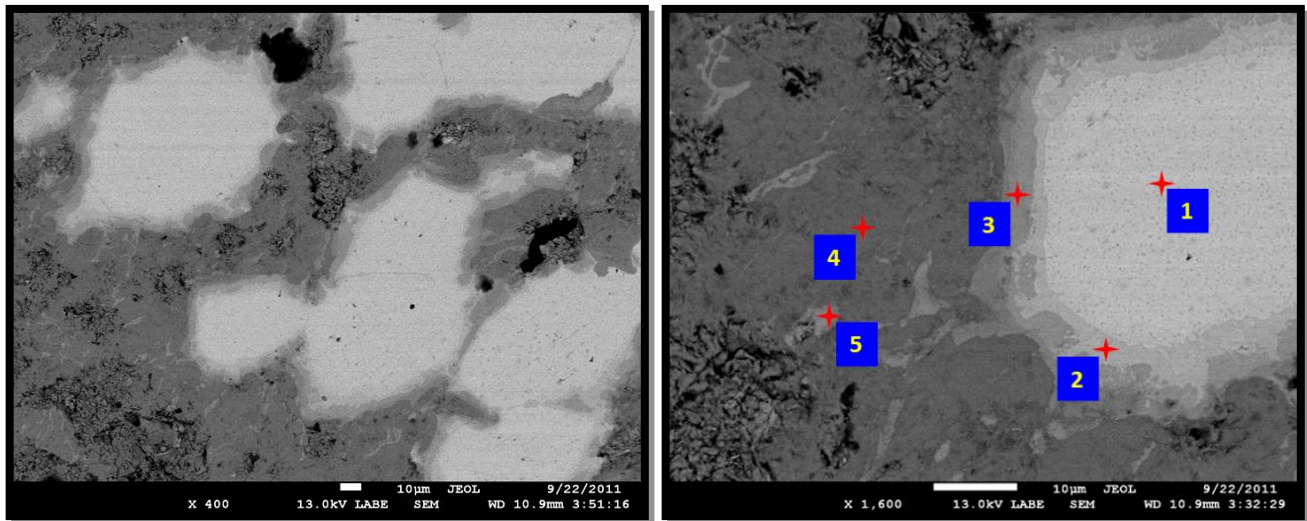
The structure of the composites were studied using Field Emission Scanning Electron Microscope (FE – SEM, Quanta 600 FEG, FEI, Oregon, USA or JSM-7500F, JEOL, Tokyo, Japan) after cross-sectioning and polishing. **Figure 7** shows the back scattering SEM images and EDS results for NiTi – Ti₂AlC sample A-14. Two phases and an interface with thickness of 4 ~ 8 μm between them could be clearly seen in the images. The EDS results show the atomic fraction of each elements C, Al, Ti and Ni in different regions. The corresponding results for the NiTi – Ti₂AlC sample A-4 and NiTi – Ti₃SiC₂ sample B-2 are shown in **Figures 8 and 9**, respectively.



Element		C	Al	Ti	Ni
	Spectrum 1	8	0	42	50
	Spectrum 2	9	13	32	46
Atom. %	Spectrum 3	18	19	38	25
	Spectrum 4	36	15	49	0

Figure 7. Back scattering SEM images and EDS results of the NiTi – Ti₂AlC composite sample A-14.

Although a reaction and diffusion layer with a thickness of 4 ~ 8 μm formed at the interface between NiTi and Ti₂AlC in the composite samples A-14 and A-2, the majority of NiTi and Ti₂AlC is intact after sintering and bonded by the reaction and diffusion interface layer. Note that same pores can be observed in the Ti₂AlC phase in Figure 7 and 8, because full densification of Ti₂AlC requires temperatures higher than used for processing composites (960 ~ 980 °C, 10 ~ 20 min and 100 MPa). The results of the density and porosity measurements in **Table 3** also show volume fraction porosity of 10.5 % for the composite sample B-2.

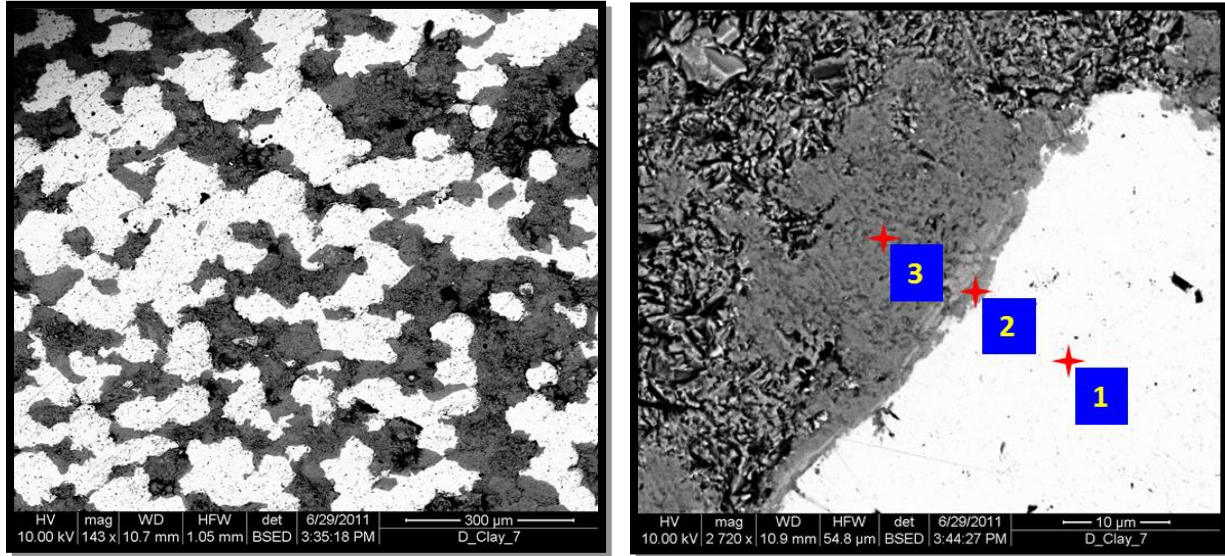


Element		C	Al	Ti	Ni
	Spectrum 1	0	0	44	56
	Spectrum 2	32.5	6.96	30.9	29.6
Atom. %	Spectrum 3	30.4	15.7	33.6	20.4
	Spectrum 4	31.2	21.4	47.4	0
	Spectrum 5	18.1	33.5	29.1	19.3

Figure 8. Back scattering SEM images and EDS results of the NiTi – Ti₂AlC composite sample A-2

The reaction and diffusion layer between in the NiTi – Ti₃SiC₂ composite sample B2 was thinner than that in the NiTi – Ti₂AlC composites, **Figure 9**, but the relative density of the former was lower than the latter. Because the densification of Ti₃SiC₂ occurs at higher temperature (see previous section), longer time or higher pressure than that of Ti₂AlC, the same processing conditions (980 °C, 10 min and 100 MPa) resulted in the higher volume fraction porosity in the NiTi – Ti₃SiC₂ composite samples when compared to NiTi – Ti₂AlC composite samples.

Although more work is still needed to process fully dense NiTi-MAX phase composites with no or little reaction between two phases, when compared FESEM images of the samples processed using SPS in **Figures 7 and 8** to that using conventional pressureless sintering in **Figure 10**, advantage of using SPSing is more than obvious. **Figure 10** clearly shows that NiTi completely reacted with Ti₂AlC composite during pressureless sintering at 1000 °C for 4 hours, while after processing NiTi-Ti₂AlC composites by SPS, **Figures 7 and 8**, majority of the NiTi and Ti₂AlC does not react and is present in the composite.



Element		C	Al	Ti	Ni
	Spectrum 1	10.24	2.14	0.18	38.19
Atom. %	Spectrum 2	40.2	-8.64	8.6	59.43
	Spectrum 3	29.8	7.74	15.27	46.41

Figure 9. Back scattering SEM images and EDS results of the NiTi – Ti_3SiC_2 composite sample B-2.

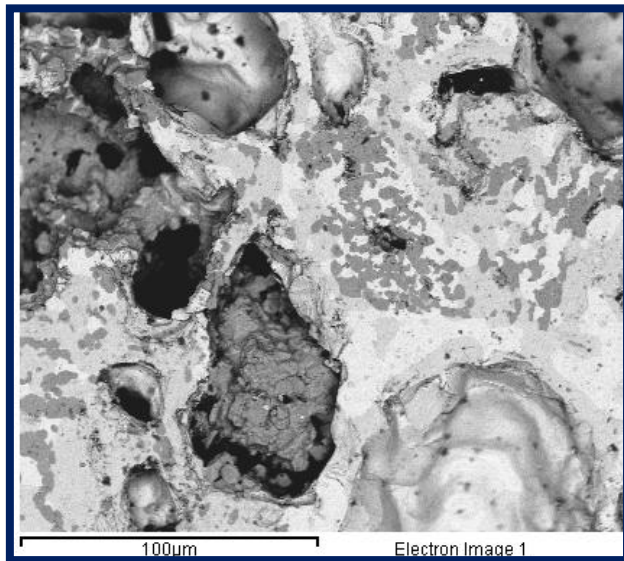


Figure 10. FE-SEM image of the NiTi- Ti_2AlC composite after pressureless sintering at 1000 °C for 4 hours.

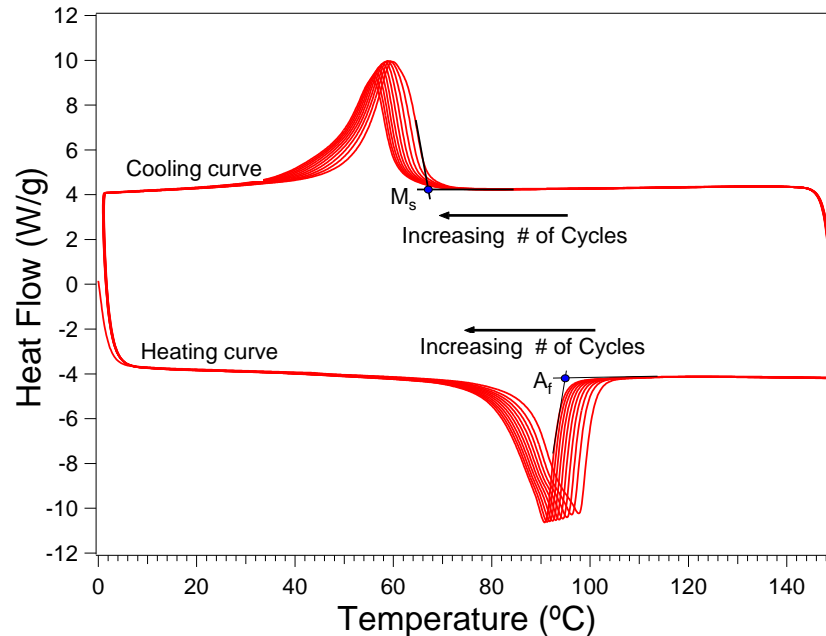


Figure 11. DSC curves of NiTi-Ti₃SiC₂ composite.

Characterization of Spark Plasma Sintered NiTi- MAX Phase Composites

Out of the various samples prepared by spark plasma sintering at different temperatures, pressures and times, two composites, NiTi-Ti₃SiC₂ and NiTi-Ti₂AlC, having lowest porosity and the smallest amount of reaction in the interfaces were chosen for characterization. NiTi-Ti₃SiC₂ composite prepared at a sintering temperature of 960°C, for duration of 20 minutes, under a constant pressure of 100 MPa had a porosity of 15.9%. On the other hand, NiTi-Ti₂AlC composite prepared at a sintering temperature of 980°C, for duration of 10 minutes, under a constant pressure of 100 MPa had a porosity of 10.6%. Differential Scanning Calorimetry (DSC) is a very important technique to study transformation behavior of materials and was employed to determine the amount of transformable NiTi phase present in the composites after sintering. NiTi, a constituent of the composites, being a shape memory alloy, transformation temperatures of the composites were also determined using DSC technique. With the help of liquid nitrogen as an accessory to the calorimeter, thermal cycling was done at heating and cooling rate of 10°C/min up to 10 cycles, counting cycling from 0 to 150°C and back to 0°C as one cycle. **Figure 11** shows the DSC curves while quantitative results of the DSC are shown in the **Table 4**. NiTi, being a shape memory alloy undergoes phase transformation from low temperature (Martensite) phase to high temperature (Austenite phase) on applying thermal energy and returns back to martensite when it is cooled. This phase transformation is accompanied by a volume change in the shape memory alloy. Phase transformation property is used to create residual stresses in the composite, thereby altering the properties of the NiTi-MAX phase composite.

Table 5. Data obtained from DSC technique for composites

Composites	Enthalpy of Transformation (J/g)		Austenite start(A_s)	Martensite start(M_s)	$A_s - M_s$	Volume percent of transformable phase
	Martensite to Austenite	Austenite to Martensite	(°C)	(°C)	(°C)	(%)
NiTi-Ti ₂ AlC	8.8	9	86	66	20	21.8
NiTi-Ti ₃ SiC ₂	16.5	16.6	90	74	16	47.87

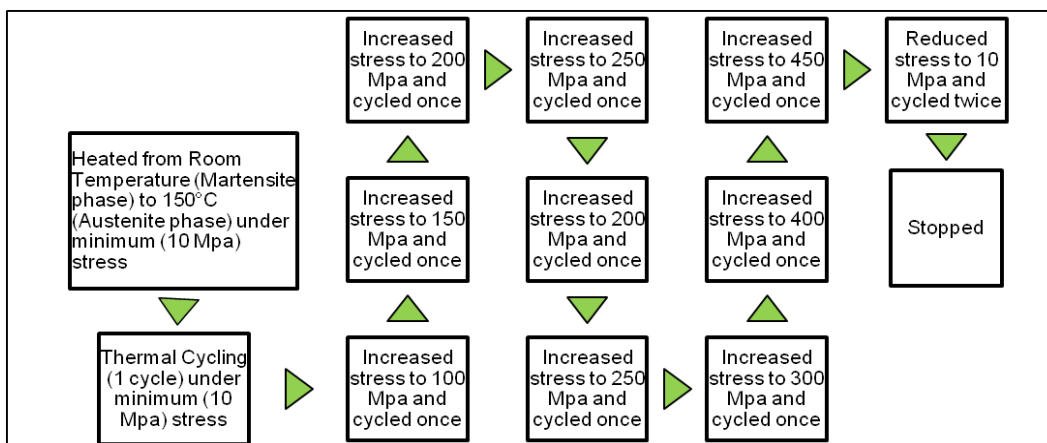


Figure 12. History of thermal cycling under compressive stress for NiTi-Ti₂AlC composite

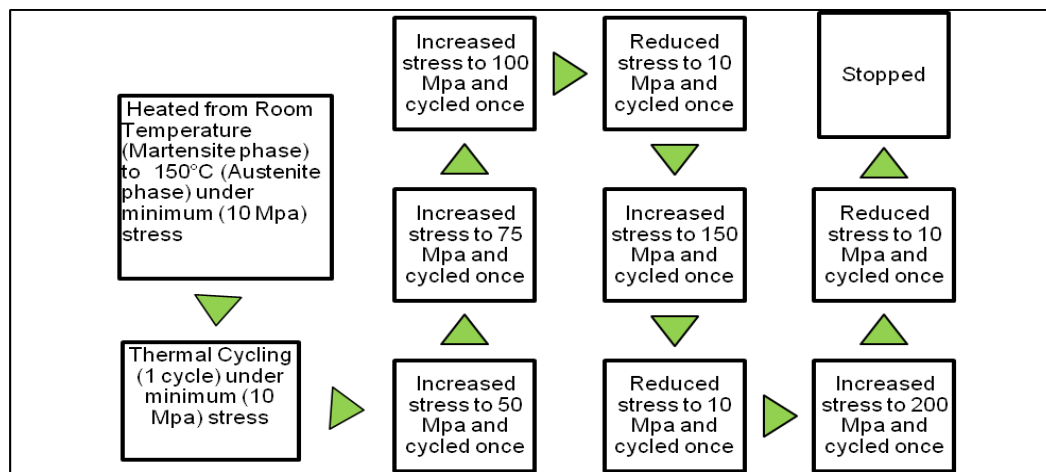


Figure 13. History of thermal cycling under compressive stress for NiTi-Ti₃SiC₂ composite

Standard compression specimens of composites were cut using wire electric discharge machining (EDM). Thermocouple was attached to the compression specimen

before it is held under minimum compressive load in a compression testing set up. Then the composite was thermally cycled from room temperature martensite phase to high temperature austensite phase under constant stress at a heating and cooling rate of 8°C/min and strain change in the composite was recorded. The stress was increased further and the temperature cycled once more while measuring the strain change associated with one thermal cycle under increasing stresses. Detailed procedure employed in the testing is illustrated in **Figure 12** for NiTi-Ti₂AlC and in **Figure 13** for NiTi-Ti₃SiC₂ composites. Results and their analysis are shown in **Figures 14-16** for NiTi-Ti₂AlC and in **Figures 17-19** for NiTi-Ti₃SiC₂ composites. It was observed that NiTi-Ti₃SiC₂ composites show very large transformation strains even at lower stresses as compared to NiTi-Ti₂AlC composites. As evident in both composites, transformation and irrecoverable strains increase with increasing applied stresses. A clear trend is observed in the evolution of transformation temperatures with increasing stress for NiTi-Ti₃SiC₂ composites which is not the case for NiTi-Ti₂AlC composites. Two way shape memory effect is observed for both the composites and NiTi-Ti₃SiC₂ composite shows much higher strains in two way shape memory than NiTi-Ti₂AlC composite.

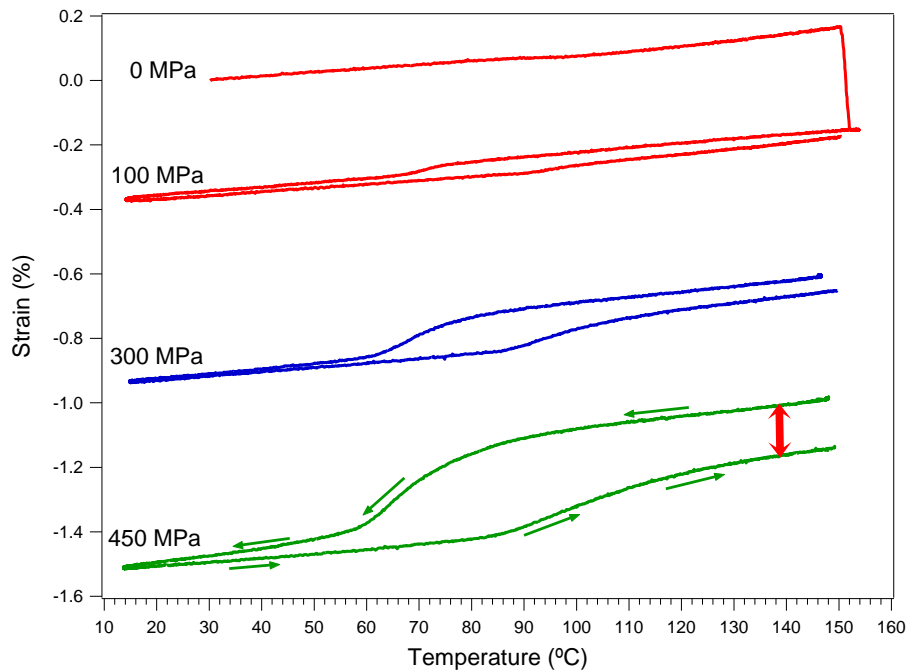


Figure 14. Strain versus temperature response of SPSed NiTi-Ti₂AlC composite under different stresses.

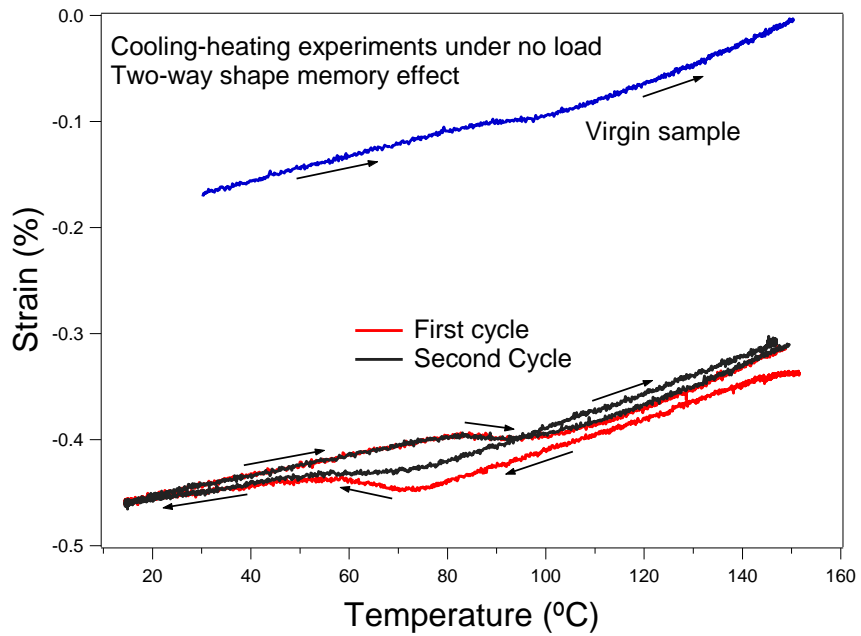


Figure 15. Strain versus temperature response of SPSed NiTi-Ti₂AlC composite under zero stress

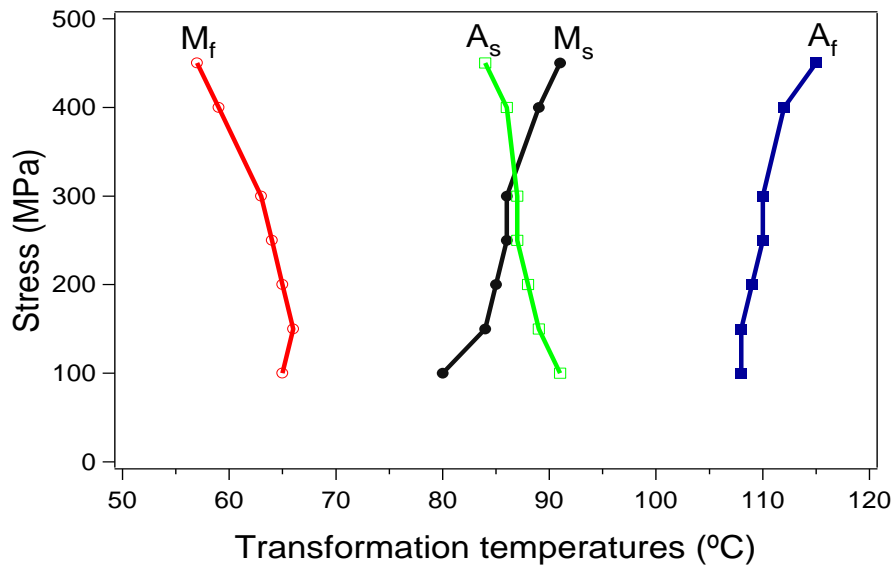


Figure 16. Evolution of transformation temperatures at different stresses for SPSed NiTi-Ti₂AlC composite

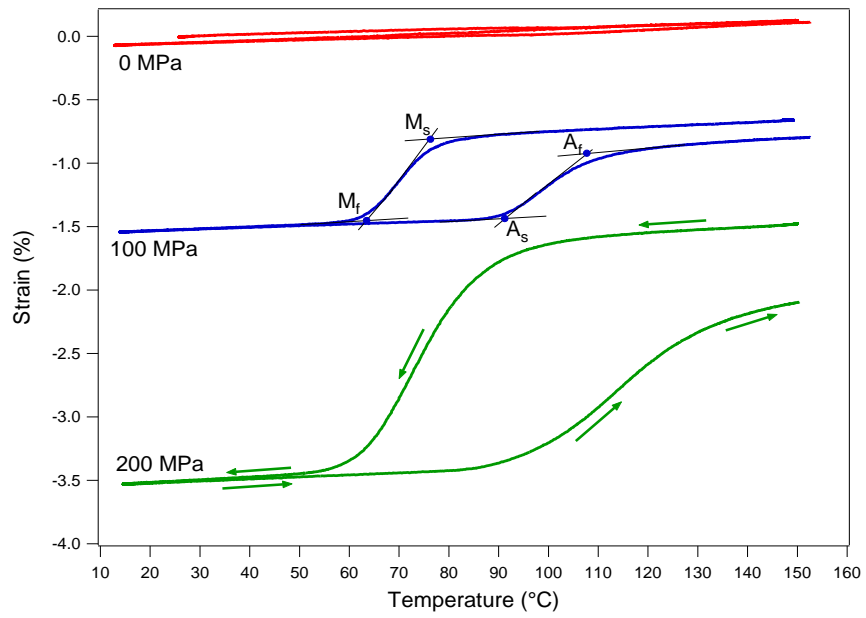


Figure 17. Strain versus temperature response of NiTi- Ti₃SiC₂ composite under different stresses.

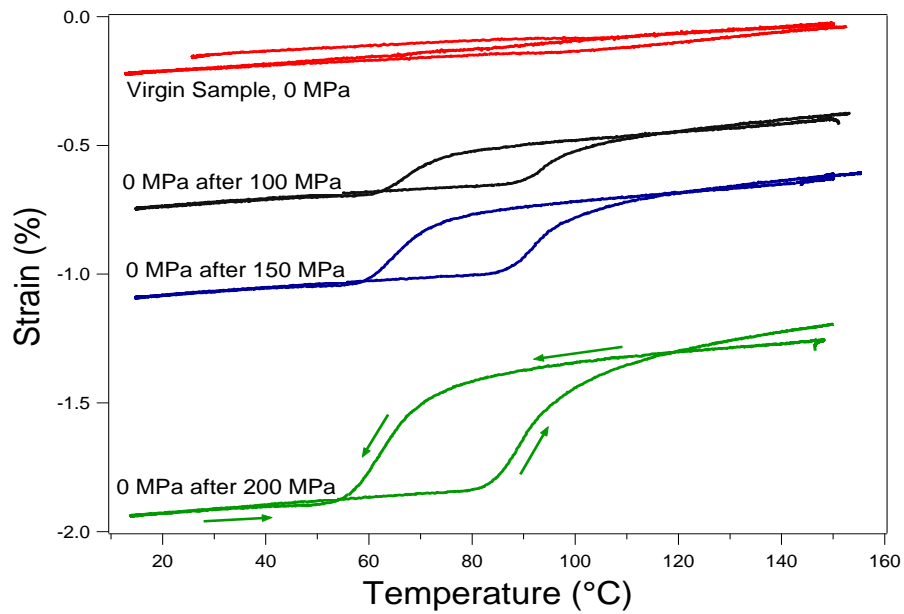


Figure 18. Strain versus temperature response of NiTi-Ti₃SiC₂ composite under zero stress

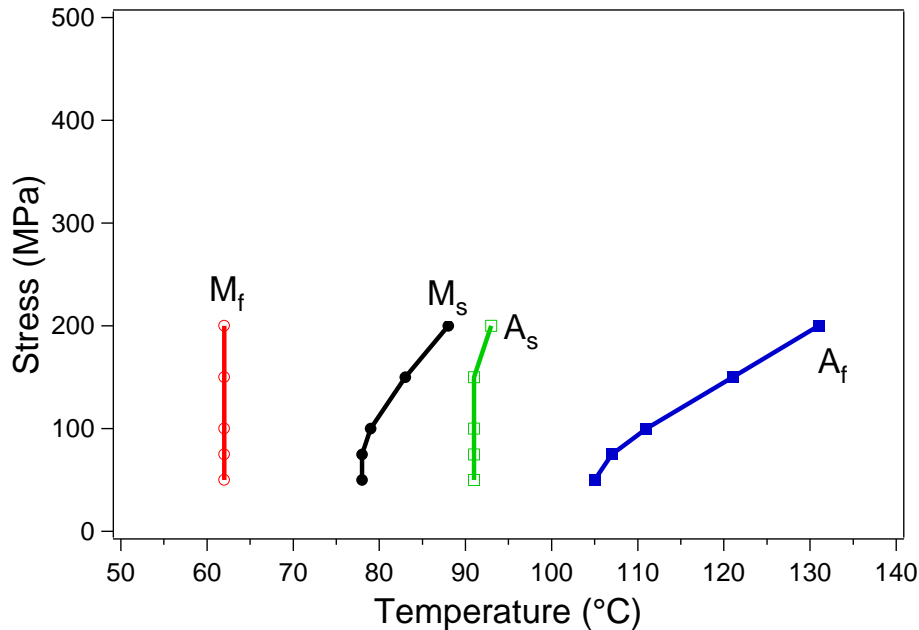


Figure 19. Evolution of transformation temperatures at different stresses for NiTi-Ti₃SiC₂ composite.

The importance of the results shown in Figures 14-19 cannot be overestimated, because they clearly show that shape memory effect can be successfully used to control type and amount of residual stresses in ceramic-composites. Figures 15 and 17 clearly show that while there is no any observable phase transformation in virgin SPSed samples during heating at zero stress, after conditioning of the composite at different stresses the phase transformation of NiTi takes place during heating even when external stress is not applied. As to the best of our knowledge, this is the first demonstration of using shape memory effect in metal alloys to control residual stresses in the ceramic-metal composites.

One of the most interesting properties of MAX phases is that they exhibit nonlinear elastic behavior and stress-strain hysteresis, as it is illustrated in **Figure 20** for Ti₃SiC₂, even after cycling for more than 100 times. It has been proposed that the mechanism responsible for this hysteretic behavior is incipient kink band formation during loading, and their annihilation during unloading. MAX phases have hexagonal close pack nanolayered crystal structure with alternating weak and strong atomic bonds. As a result of their unique crystal structure, they are stiff like other ceramics, however, under loading basal and only basal plain dislocations can form. When a load is applied, dislocation walls of opposite sign form through width of the grain forming incipient kink bands. If the load is further increased or temperature is raised above the materials brittle to ductile transition (~ 1000°C) the dislocation walls may grow and become pinned by grain boundaries causing permanent kinking. However, if the critical loading is not exceeded, incipient kink bands can collapse upon unloading. In the latter case, the material will return to its unloaded shape, dissipating large amount of mechanical energy due to internal friction of dislocation in the process. It is this energy dissipation that is of interest and our subject of study through cyclic compression testing.

Mechanical cycling of SPSed MAX phases and NiTi-MAX phase composites was performed in MTS Insight testing system with 30 kN load cell, to determine if generation of residual stresses in the composites can increase mechanical damping. Compression samples 3.5 mm x 3.5mm x 7mm were cut by EDM with special care to ensure parallel surfaces, critical for compression testing. The samples were tested under load control with loading/unloading rate of 60 N/s. A custom made extensometer with 3mm gage length was use for accurate strain measurements. Each sample was cycled twice at initial stress value of 50 MPa and then this process was repeated six times, each time at 25 MPa higher than the previous set point such that the stress level tested were 50, 75, 100, 125, 150, 175, 200 MPa.

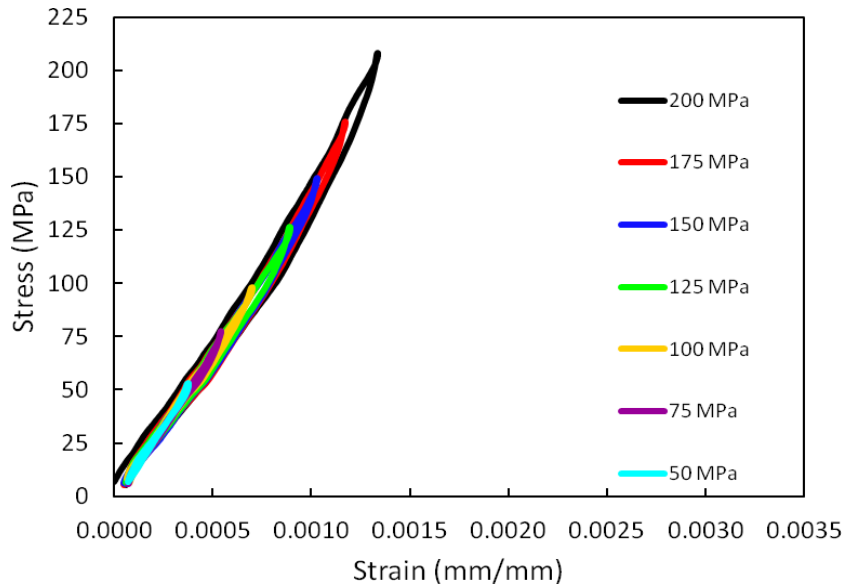


Figure 20. Cyclic stress- strain behavior of Ti_3SiC_2 at various stress levels.

The cyclic stress-strain behavior of pure Ti_3SiC_2 as synthesized by SPS with parameters previously discussed can be seen in **Figure 20**. However, addition of 50% NiTi, shape memory alloy to Ti_3SiC_2 significantly enhances the energy dissipation as it can be seen from the larger size of the hysteresis loops of the composite in **Figure 21**. To analyze better the dissipation capabilities of these materials, the energy dissipated per unit volume, W_d , with units of MJ/m^3 , was calculated by integrating the area inside the hysteretic loop and plotting it as a function of maximum applied stress squared, **Figure 22**. From this figure we can see that the NiTi- Ti_3SiC_2 composites exhibits significantly larger mechanical damping when compared to the pure Ti_3SiC_2 . However, NiTi- Ti_2AlC composite does not enhance the energy dissipation capabilities Ti_2AlC , a condition that is presently being analyzed. Although, more work is needed to fully understand observed differences in the mechanical damping between MAX phases and their corresponding composites with NiTi, it is believed that the reason for higher damping in NiTi- Ti_3SiC_2 lies in the compressive residual stresses that are induced in Ti_3SiC_2 . In other words, because of the compressive residual stress in MAX phases, the

actual stress in compression is larger than the applied stress and results in more intensive incipient kink band formation.

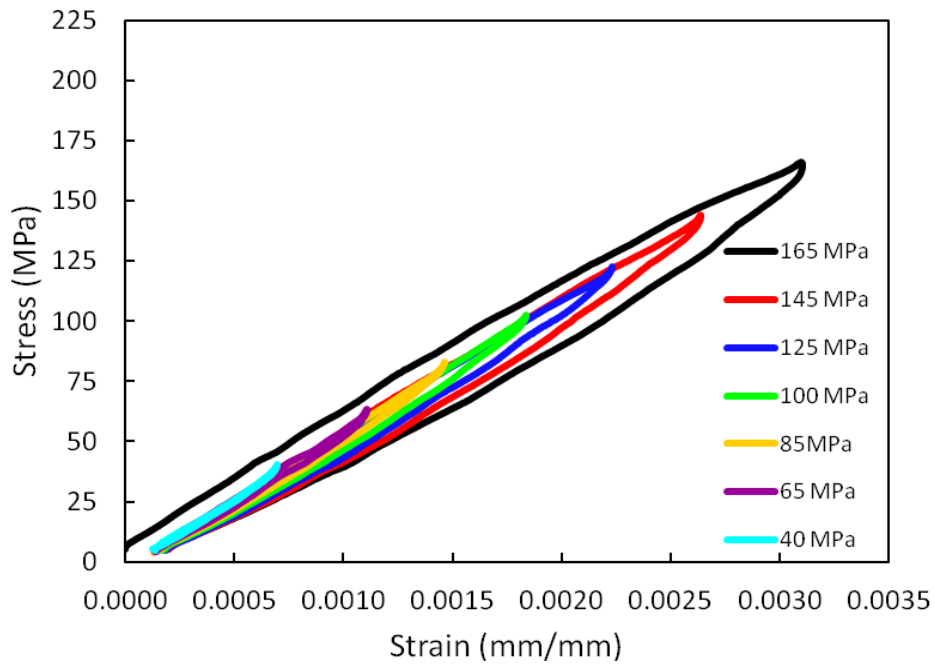


Figure 21: 50% Ti_3SiC_2 - 50% NiTi sintered 10 min at 980°C & 100 MPa.

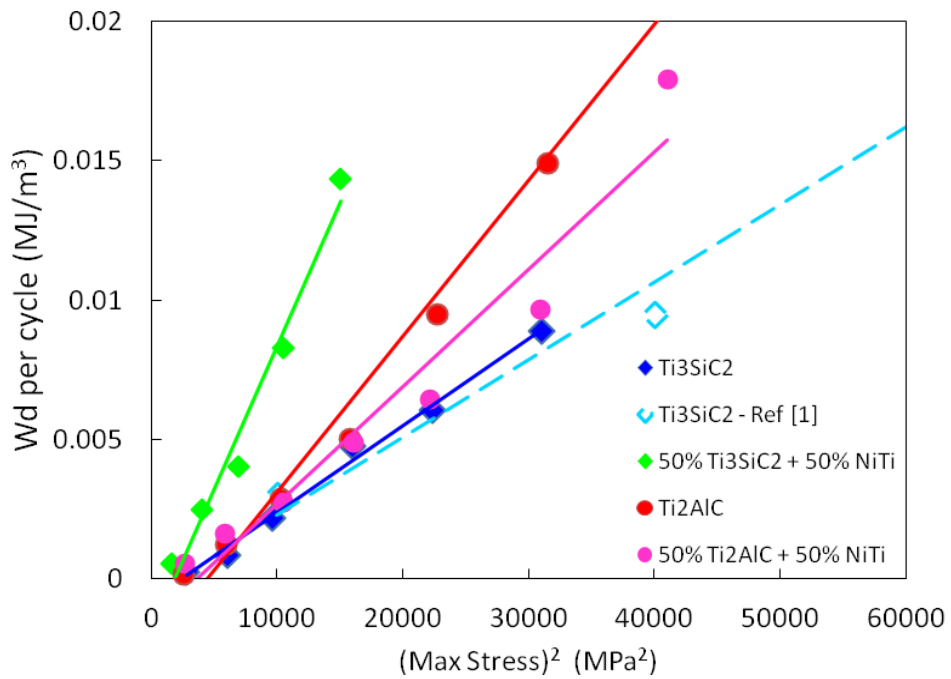


Figure 22. Energy dissipated per unit cycle as a function of applied stress.